IJE TRANSACTIONS A: Basics Vol. 32, No. 1, (January 2019) 153-161

International Journal of Engineering

Journal Homepage: www.ije.ir

A Numerical Simulation of Vanadium Redox Flow Batteries

P. Hasannasab, A. A. Ranjbar*, M. Shakeri

Mechanical Engineering Department, Babol Noshirvani University of Technology, Babol, Iran

P A P E R I N F O

Paper history:
Received 30 November 2018
Received in revised form 29 December 2018
Accepted 03 Januray 2019

Keywords:
Flow Fields
Pressure Loss
All Vanadium Redox Flow Battery
Numerical Simulation

A B S T R A C T

The recent penetration of renewable sources in the energy system caused a transformation of the needs of the distribution system and amplified the need of energy storage systems to properly balance the electricity grid. Among electrochemical energy storage devices, all vanadium flow batteries are those of the most promising technologies due to their high efficiency, long lifetime, reliability and independence between installed power and storage capacity. Oppositely, the low energy density and the high costs are preventing this technology from spreading at commercial level, even if many are the opportunities of improvement. In this article, a serpentine flow fields are tested using a numerical simulation for the all vanadium redox flow battery. The development of a three dimensional model for the cathode of a vanadium redox flow batteries is presented. The results were discussed in terms of the uniformity of the reactant distribution, overpotential, velocity and state of the charge through the cell.

***doi**: 10.5829/ije.2019.32.01a.20*

NOMENCLATURE

d	Diameter	**Greek symbols**	
C	Concentration (mol/m^3)	μ	Viscosity (kg/ms)
F	Farady's constant (C/mol)	ε	Porosity
H^+	Hydrogen ions	υ	Volume
I	Current (A)	ρ	Electrolyte density (kg/m^3)
K_{KC}	Kozeny-Carmen constant	α	Charge transfer coefficient
k	Reaction rate constant (m/s)	β	Degree of dissociation
K_p	Hydraulic permeability (m^2)	η	Overpotential (V)
$K_\emptyset$	Electro kinetic permeability (m^2)	**Sup/subscripts**	
M	Molarity	*acid*	Acid
p	Pressure (Pa)	*f*	Fiber
SOC	State of charge	*F*	Fixed membrane structure
T	Temperature (K)	*i*	Species
t	Time (s)	*II*	Bivalent vanadium ions
u	Ion mobility	*III*	Trivalent vanadium ions
VO_2^+ *or* V^{5+}	Pentavalent vanadium ions	*IV*	Tetravalent vanadium ions
VO^{2+} *or* V^{4+}	Tetravalent vanadium ions	*V*	Pentavalent vanadium ions
V^{3+}	Trivalent vanadium ions	*tot*	Total
V^{2+}	Bivalent vanadium ions	*van*	Vanadium
		void	Fluid

*Corresponding Author Email: *ranjbar@nit.ac.ir* (A.A. Ranjbar)

Please cite this article as: P. Hasannasab, A. A. Ranjbar, M. Shakeri, A Numerical Simulation of Vanadium Redox Flow Batteries, International Journal of Engineering (IJE), IJE TRANSACTIONS A: Basics Vol. 32, No. 1, (January 2019) 153-161

1. INTRODUCTION

Electrical energy storage system has become a major concern worldwide due to rapid growth in renewable energy [1]. Electricity generated by renewable energy sources like wind and photovoltaics, is inherently intermittent. Dhassa *et al.* [2], investigate on the effect of temperature on photovoltaic cells. the influence of thermal effect on the solar system is considered and its influence on the performance of the operation, fill factor, open circuit voltage, and short circuit current, band gap level of various semiconductor materials, output power and efficiency are analyzed.

A high Energy Storage System (ESS) technology is needed in order to balance the demand and the supply in renewable energy systems. Redox flow battery (RFB) technologies have proved to be beneficial with applications including remote area and back-up power supplies, distributed power generation, load leveling and peak shaving [3]. Between various RFB systems, the all-vanadium redox flow battery (VRFB) has shown the greatest potential for large scale energy storage applications with flexible design, scalability, quick response, tolerance to deep discharge, long cycle life, high energy efficiencies of over 80% in large installations and active thermal management [4]. The commercial development and economic incentives associated with energy storage using redox flow batteries (VRFBs) is summarized by Kear *et al.* [5] and Skyllas-Kazacos *et al.* [6]. In addition, several technical aspect and underlying physical processes of all vanadium redox flow batteries are given in the recent reviews of Weber *et al.* 7]. The extremely large capacities possible from vanadium redox batteries make them well suited to use in large power storage applications such as helping to average out the production of highly variable generation sources such as wind or solar power, helping generators cope with large surges in demand or leveling out supply/demand at a transmission constrained region. Their extremely rapid response times also make them superbly well suited to uninterruptible power supply type applications, where they can be used to replace lead–acid batteries and even diesel generators. Also the fast response time makes them well-suited for frequency regulation. Economically neither the UPS nor frequency regulation applications of the battery are currently sustainable alone, but rather the battery is able to layer these applications with other uses to capitalize on various sources of revenue. Also, these capabilities make vanadium redox batteries an effective all-in-one solution for micro-grids that depend on reliable operations, frequency regulation. In recent years, mathematical models of the vanadium flow batteries have been developed to predict and investigate the performance of the VRFB systems ranging from two-dimensional and three-dimensional models to simple zero dimensional lumped parameter models. A comprehensive review of state-of-the-art flow battery modeling is given by Xu and Zhao [8]. Kim *et al.* [9] study on performance and efficiency of all-vanadium redox flow batteries and relationship between ion concentration and parameters in the system. They found that as flow rate increases, the energy efficiency slightly increases, because faster flow rates can deliver more vanadium ions from the reservoir. The energy efficiency decreases according to current density, because large current results in large amount of ohmic loss of membrane. When the size of active area increases, the energy efficiencies remain constant, however, the cycle time decreases. Due to high level of complexity associated with multi-dimensional models, they cannot be used as control and monitoring tools or stack models for predicting the long term performance of the VRFB cells. Yin *et al.* [10] proposed a 3D model for an interdigitated flow field with two different designs. Their focus was on the how to build the inlet, whether to use a single-inlet configuration or a multi-inlet one. Simulations were structured in the model are to study the distributions of fluid pressure, electric potential, current density and overpotential during operation of VRFB cell. There are similarities among the model developed for redox flow batteries and fuel cell models, namely polymer–electrolyte (PEMFC) and direct-methanol. Although there are numerous articles on the modeling of PEM fuel cells, however less attention was paid to modeling all vanadium redox flow batteries. In recent years, several mathematical models of the VRFB have been developed to predict and investigated in the performance of the VRFB systems ranging from two-dimensional and three-dimensional models to simple zero dimensional lumped parameter models. A comprehensive review of state-of-the-art flow battery modeling is given by Xu and Zhao [11]. They had a short review on multi-dimensional modeling and the simulation of VRFB systems will be given. Shah *et al.* [12], were the first development of a transient, two-dimensional model for VRFBs based on conservation principles (mass, momentum and charge), incorporating the fundamental modes of transport for the charged species and water accounting for the overall half-reactions (i.e., reduction and oxidation of vanadium species) and the resulting transport of vanadium ions, hydrogen ions, water, and sulfuric acid. This transport model was combined with a kinetic model to simulate the performance of the all-vanadium RFB. This model was validated against the experimental data and was used to study the effects of variations in concentration, electrolyte flow rate and electrode porosity. However, several key phenomena such as the crossover of vanadium ions through the membrane, side reactions, thermal effects, and electron transport were neglected in

their model. Later, You *et al.* [13], based on the VRB model which was developed by Shah *et al.* [12], and applied a simplified two-dimensional stationary model to study the effects of applied current density, electrode porosity and local mass transfer coefficient on the cell performance. The transient terms in the governing equations were eliminated by pre-calculations of the Nernst potentials of the positive and negative electrodes at any given time. In order to prove the validity of the model, a simple experiment was carried out. This study completed some aspects that were not discussed in literature [12], and puts forward different views on the effects of electrode porosity. The model results indicated that bulk reaction rate depends on the applied current density. The transfer current density and over-potential increased almost twice as the applied current density doubled. A decrease in electrode porosity led to a more rapid depletion of the reactant concentration, a higher integral average value of the transfer current density and a more uniform distribution of the over-potential. The local mass transfer coefficient only affected the value of the over-potential. Pugach et al. [14] investigated on the effects of crossover in this field. They proposed a control-oriented zero dimensional model of VRFB cell and performed precise simulation of crossover. They elaborate an analytical solution for crossover flux with all three modes. The influence of these phenomena on the capacity decay was systematically analyzed, revealing considerable impact of convection component, which dominates under diffusion and migration and mainly responsible for observed capacity loss. The model allows to simulate main characteristics of VRFB systems (such as battery voltage, state of charge, charge/discharge time and capacity decay due to crossover) with high accuracy. The model was validated with experimental data in the wide range of current densities (40–100 mA cm^{-2}), and the results demonstrated good agreement with experiments having an average error within 5% range. According to literature review, few works have been reported regarding the utilization of different flow fields for redox flow batteries. Here, in this paper, we intend to further examine the possibility of gaining VRFB performance improvement using flow fields and numerical simulation. We intend to develop a 3-D model for VRFB which considers the cross over phenomena, non-isothermal effects and incorporates an electrochemical transport-thermal coupled model for VRFBs. The 3-D simulation results presented in this study clearly address detailed impacts of the flow fields on multi-dimensional species distributions as well as on overall thermal-electrochemical behaviors of VRFBs. López-Vizcaíno *et al.* [15] simulated the performance of VRFB for the storage of electricity produced in photovoltaic solar panels in two different mode. They tested a VRFB simulating solar panel in charging mode and checked these type of batteries which was charged in galvanostatic mode at constant current. Their results indicate that VRFBs are suitable devices for the storage of the electricity produced in photovoltaic solar panels. Suresh *et al.* [16] optimized the cell configuration utilizing various carbon felts for obtaining better performance in zinc-bromine redox flow battery. They observed the reaction kinetics of both Zn and Br which are enhanced when used in different cell configurations with carbon felts. Results showed redox flow cells carbon felts on both half-cells showed improved performance in compare to other cell configurations. Yan *et al.* [17] found that dynamics of the stack can be controlled by controlling that of the storage tanks. They also realized larger tank surface area can limit stack temperature growth in the long run. Li *et al.* [18] proposed a model based non-linear optimization approach to obtain the optimal charging current and electrolyte flow rate trajectories as functions of time for a vanadium redox flow battery. The optimization objective is formulated to minimize the total energy consumption of the battery and pumping system. Bhattacharjee *et al.* [19], developed an efficient thermal management system for VFRB. They designed a model to forecast the stack temperature and dynamically optimize the flow rate. They observed that at a lower flow rate of 180 ml/s the stack temperature during fast charging and discharging at the rate of 60A rises up to 47 °C which is well above the specified safe limit of operating temperature of VRFB and leads to incomplete charging due to premature thermal shut down of the system. Particularly important for this work is as it uses a three-dimensional model to understand the fluid dynamic behaviour of a flow battery for the flow field design. The main advantage of having a full 3D model is to have information about the quantities in planes or in volumes that consider the whole cell. Other important differences from the model presented are the dimensions of channels and electrode and the molarity of the inlet solution. It has to be reported that in the literature there are also models that do not solve the electrochemical part of the cell, limiting their action just to the fluid dynamic behaviour and the characterization of the relation between the flow regime and overpotential.

2. MATHEMATICAL MODELLING

Mathematical modelling helps to understand processes and plays an important role in process design, optimization and control. The fitting procedure has brought to the determination of a set of parameters used throughout the work and gave the opportunity to understand which are the most influencing phenomena and how they are modelled using the constitutive equations of the electrochemical cell. The weight of the parameters on the cell behaviour was clarified and a

procedure to solve together electro chemistry and fluid dynamics was developed. A three dimensional code has been developed. This model solves both electrochemistry and fluid dynamics. Such level of detail allows the visualization of the phenomena that occur in the porous electrode and in the channels. What emerges is that the flow in porous medium is not easy to be modelled and its link with electrochemical quantities is complicated: the solid part of the domain is not physically present in the models. In this work flow through porous medium was modelled using the default template in ANSYS Fluent. The study of flow through porous media is explained in details in literature [20]. By considering a volume of porous medium the porosity is defined as the ratio of the fluid volume over the total volume:

$$\varepsilon = \frac{\upsilon_{void}}{\upsilon_{tot}} \tag{1}$$

A distinction is made between an average taken with respect to a volume element υ of the medium (incorporating both solid and fluid material) and one taken with respect to a volume element consisting of fluid only.

The first quantity has been given various names, by different authors, such as filtration velocity, superficial velocity, Darcy velocity, and volumetric flux density. This is not the only choice and taking an average of the fluid velocity over a volume of fluid one gets the intrinsic average velocity called also physical velocity. The link between them is straightforward:

$$V_{physical} = \frac{V_{superficial}}{\varepsilon} \tag{2}$$

In this work it is preferred to model fluid flow according to a physical velocity formulation when solving continuity and momentum equations since the values of the velocity in the porous medium are important for our purposes.

$$\nabla.[-pI + \frac{\mu}{\varepsilon}(\nabla u + (\nabla u)^T) - \frac{2\mu}{3\varepsilon}(\nabla u)I] - (\frac{\mu}{\kappa} + \beta_F |u|)u = 0 \tag{3}$$

This formulation of the momentum equation adds two momentum sinks, one proportional to velocity and the other proportional to the square of the velocity. The determination of the coefficient of the Forcheimer is hard and it is difficult to find adequate literature.

Also, the Darcy term is sufficient to model the pressure drop through the electrode: velocities values are limited in the porous medium (the order of magnitude is not larger than 10^{-1} m.s^{-1} in all working conditions). In the range of flow rates analyzed (from 10 to 60 mL.min^{-1}) the value of this ratio was never below 30, justifying the choice of neglecting the Forcheimer term.

Permeability values are crucial for the correct modelling of the battery and their value is determined by the properties of the electrode and by its compression. For simplicity the medium is treated as isotropic. This fact is not guaranteed in the reality as the electrode might not be homogeneous and behave differently according to the direction taken into account. Particularly, for this kind of application, it is not strange to forecast a different behaviour of the electrode between the in-plane direction and the through-plane direction but, since in the literature few detailed studies are present, the medium is treated as isotropic.

Many authors calculate permeability from the mean fiber diameter and the porosity from the Kozeny-Karman relation:

$$K = \frac{{d_f}^2 \varepsilon^3}{K_{KC}(1-\varepsilon)} \tag{4}$$

Where K_{kc} is the Kozeny Karman constant, usually 180. In porous media compression does not change the shape of the fibers but reduces the void space. A correction for porosity:

$$\frac{t_1}{t_0} = \frac{1-\varepsilon_0}{1-\varepsilon_1} \tag{5}$$

Similarly permeability decreases increasing compression and to quantify this trend a correlation was used:

$$\frac{K}{K_{uncomp}} = 1.6\frac{t}{t_{uncomp}} - 0.6 \tag{6}$$

The value for permeability was found therefore to be $K = 1.75e^{-11}$ m^2, notice how this value is one order of magnitude lower than the value used in the bi-dimensional model. This is reasonable considering the geometry of the 2D model: the pressure gradient is expected to be mainly distributed along the channel direction and it is not supposed to have a component that is pushing the fluid actively into the porous medium. For this reason, in order to have an effective access of the reagents to the electrode a lowered value for permeability is required. Regarding the fluid dynamic condition, the model of the flow is laminar. This choice is coherent with the velocity values present in the flow fields and with the literature.

To check the validity of this hypothesis Reynolds number based on the equivalent diameter of the channel is calculated and reported for the highest flow rate considered. The velocity chosen to calculate Reynolds is the maximum in the channel and for the highest flow rate presented in the work (100 ml.min^{-1}) the value of a dimensional group is around 600. Since the values are well below the transition Reynolds number the choice of

laminar flow is justified. Boundary conditions are set to create a stationary voltage controlled model. At the inlet, mass fraction are imposed from the value of the state of charge and the molarity of the acid solution. The link between concentration and mass fraction is stated as following:

$$X_i = \frac{C_i M}{\rho} \qquad [kg_i / kg_{tot}] \tag{7}$$

The equations that link molarities and state of charge to the concentration of the solutions are:

$$c_{vo^{2+}} = (1 - SOC) M_{van} \tag{8}$$

$$c_{vo_2^+} = SOC M_{van} \tag{9}$$

$$c_{H+} = M_{acid} - M_{van} + M_{van} SOC \tag{10}$$

$$c_{HSO_4^-} = M_{acid} + M_{van} \tag{11}$$

To describe the relative amount of vanadium ions with different valences, we define the SOC as follows:

$$SOC = \left(\frac{c_{V(II)}}{c_{V(total)}}\right)_1 = \left(\frac{c_{V(II)}}{c_{V(total)}}\right)_2 \tag{12}$$

Velocity is also imposed at the inlet to control the flow rate. For sake of simplicity a uniform distribution is imposed whose value is derived from the volumetric flow rate. For the serpentine channel a velocity of 0.53 $m.s^{-1}$ gives 20 $ml.min^{-1}$. At the outlet, pressure is set at a null value to create a pressure reference. On the ribs between the channels a value of the solid potential is fixed, while at the interface of the membrane where the anode should be the liquid potential is set to zero.

3. DOMAIN AND MESHING

Since the geometries in this work are characterized mainly by regular shapes, the choice for the mesh is to use quadrilateral cells. The portion of the domain in which velocity gradients are expected to be higher are meshed with higher accuracy, as well as the porous electrode domain since in this area there are more equations to be solved. The different parts of the domain are shown and the geometric characteristics are: the area of the cell is 25 cm^2, the channel has a side of 0.8 mm and the rib size is also 0.8 mm. The serpentine geometry and its details are shown in Figures 1 and 2. Notice how the inlet and the outlet are on the same side of the domain. A dedicated procedure is implemented to build the polarization curve. Each point is calculated increasing progressively the under relaxation factors for the constitutive equations.

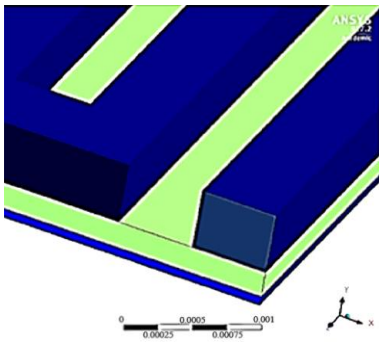

Figure 1. Details of 3D model

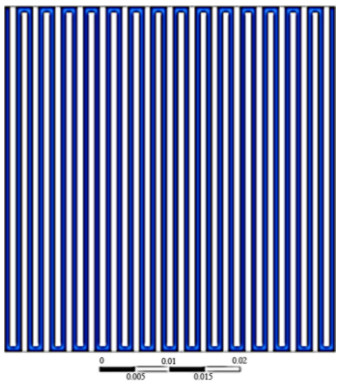

Figure 2. Serpentine geometry

4. RESULTS AND DISCUSSION

Parameters for the model are in Table 1. The performance is analyzed through polarization curve just during the phase of discharge for sake of convenience due to the long computational time needed by the simulations: each point to reach convergence needed 3000 iterations that is nearly 30 minutes of calculation on a 16 cores cluster.

To get a polarization curve two hours are needed. The trend of real curves as shown in Figure 3, is not perfectly the same of the models but it is reasonable since no dedicated fitting procedure was directly performed on this model. The variability of the performance with respect to the flow rate is forecast by the model even if at low flow rate there is underestimation of the performance. These differences have to be kept into consideration when dealing with reasoning.

Coding a new model required much effort and during the first attempts mono dimensional trends have been very useful to understand if the constitutive equation were written correctly and if the model was coherent with the 2D one. Figures 4 and 5 show liquid and solid potential in y-direction lines are chosen at the center of a channel at the center of the cell x = 0.0247m.

TABLE 1. Parameters used in the simulations

Parameter	Value	Unit
$D_{V^{4+}}$	3.9×10^{-10}	m^2/s
$D_{V^{5+}}$	3.9×10^{-10}	m^2/s
D_{H^+}	9.312×10^{-9}	m^2/s
$D_{HSO_4^-}$	1.33×10^{-9}	m^2/s
$D_{SO_4^{2-}}$	1.065×10^{-9}	m^2/s
T	295	K
F	96485.3365	C/mol
R	8.314472	$J/(mol.K)$
Q_1	3.45×10^{-7}	m^3/s
υ_1	0.53906	m^3/s
Q_2	1.76×10^{-7}	m^3/s
υ_2	0.2700	m^3/s
ρ_{sol}	1350	kg/m
μ_{sol}	0.005	$Pa.s$
α	0.5	-
ε	0.8588	-
a	3.5×10^{4}	m^{-1}
K	40×10^{-11}	m^2
r_p	32×10^{-6}	m
k_0	1.8×10^{-6}	m/s

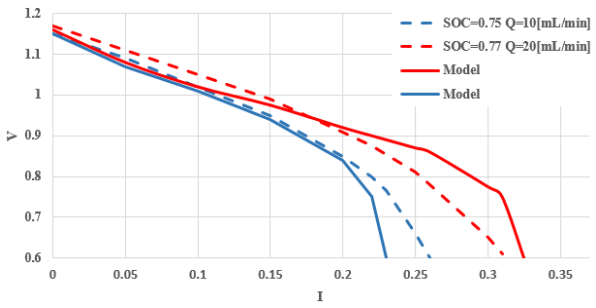

Figure 3. Comparison of the performance of the real cell with the model for *Sigracet 10 AA* electrode

Various lines are chosen and their position along the z-direction are shown in the legends. The z-direction is along the channels the y-direction is from the membrane to the channels while the x-direction is from the inlet to the outlet. The working condition of the battery chosen is a discharge one with 20 ml.min^{-1}, a state of charge is 0.77 and a potential is 0.75 V.

This gives a current density of approximately I = 0.3 A.cm^{-2}. One may say that the trends of liquid and solid

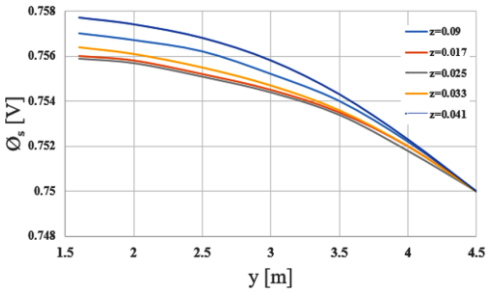

Figure 4. Trends of solid potentials in y-direction

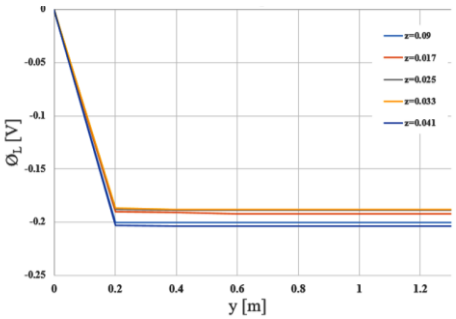

Figure 5. Trends of liquid potentials in y-direction

potential are in line with the bi-dimensional model. On one side this is true as concavities and trends with respect to the y-direction are coherent with the 2D-model.

On the other side, the three-dimensional model shows that there is not such growth of the potential with respect to the longitudinal direction of the channel ion. The initial part and the final part of the channel behave differently from the center of the cell and it is a sign that three-dimensional effects are influencing the cell behaviour.

In order to have a first insight in the cell the state of charge is shown using contours in a plane that is at half height of the porous electrode. The inlet is in the top-right corner while the outlet is in the top-left corner.

Showing the trend of state of charge is particularly wise as it allows to visualize the concentration of both the vanadium species in the domain. Several information can be withdrawn from Figure 6. The first thing is related to the behaviour of the state of charge along the area of the cell, from the beginning to the end of the cell the state of charge decreases and this is coherent with a discharge condition. Moreover, there is a very marked no uniformity when moving from under one channel to a zone under the following one. These zones have a slightly higher state of charge with respect to the nearby zones and are located under the beginning of a rib. The item which is more at the center of the cell it seems like there is an area of the cell in which the state of charge varies smoothly.

Some explanations to the trends of the state of charge are provided by the reaction rate.

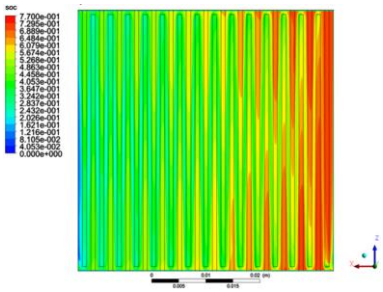

Figure 6. State of charge on a plane at half the height of the electrode

This quantity is influenced by both concentration and potentials' distributions. Figure 7 testifies how there are some zones under the rib where the rate is much higher than in the adjacent one.

A detail of the variation along the y direction of the reaction rate is shown in Figure 8 and it is visible how some zones, corresponding to the zones that are under the rib, experience a higher rate.

Since electrochemical quantities vary in such way one may ask how the fluid dynamic flow field is shaped in the porous medium and the answer is shown in Figure 9. The reported quantity is the velocity in the porous medium on a plane at half of the height of the electrode. What is clear is that the fluid is very slow in the porous medium and the magnitude of velocity is not higher than 5 percent of the channel velocity and this gives values for the velocity in the order of 0.02 $m.s^{-1}$. It has been calculated also the same variable on a XZ plane very close to the channel interface and the value of velocity did not reach 10 percent of the velocity in the channel.

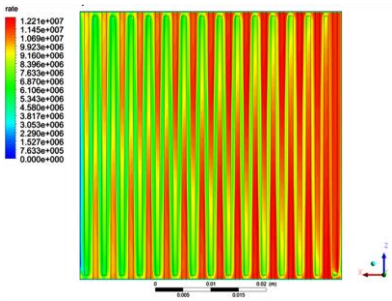

Figure 7. Reaction rate on a plane at half the height of the electrode

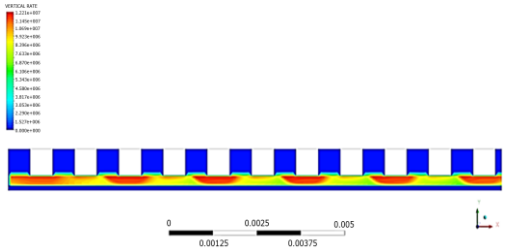

Figure 8. Reaction rate on a XY plane at Z = 5 mm from the inlet

Another interesting fact is that there is higher velocity in certain zones of the domain that are under the rib. A better visualization is done in Figure 10, where the ratio of the local velocity to the velocity in the channel is proposed. The quantity is shown on three x-directed lines, the first line is in the higher part of Figure 9 at a distance of 5 mm from the inlet, and the second is in the center of the cell, while the last is in the lower part of Figure 9.

The entity of the scaled velocity is below 5 percent and its values are lower in the center of the cell (red curve) than in the initial and final part. Considering the phenomenon along the z-direction, due to the geometry of the cell the under the rib fluxes will not be in the same position along the x-direction and this is testified by the difference of the yellow and the blue line. What is more inlet and outlet influence the fluxes in a region close to them, as seen by the blue curve. This variability anyway is not peculiar of the porous electrode but also the channel velocity experiences such decrease in the central part of the cell, while close to the curves the fluid accelerates as testified by Figure 11. This figure compares the scaled velocity for a plane at mid height of the channel and one at mid height of the porous medium, the domain chosen is the central part of the cell in the x-direction. Under the rib fluxes arise from the fact that the flow is forced to go through the minimum resistance path. Close to the curve part of fluid passes under the rib as the pressure drop associated to the electrode is much smaller than the pressure drop associated with the length of the channel and a curve.

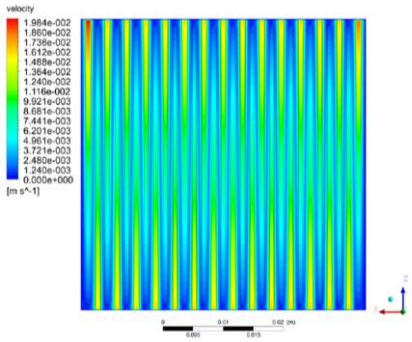

Figure 9. Velocity distribution on a plane at half the height of the electrode

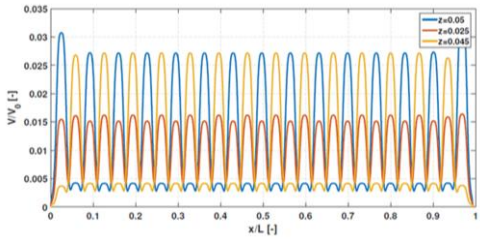

Figure 10. Under the rib fluxes on a plane at half the height of the electrode

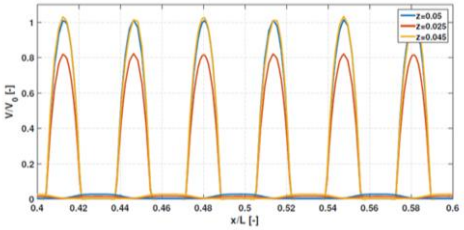

Figure 11. Under the rib fluxes and channel velocity on a plane at half the height of the electrode

What happens is that the pressure drop in the porous electrode is mainly linear with velocity while the pressure drop in the channel and particularly in the curve is proved to scale quadrilateral with velocity. For a given flow rate and hence for a given velocity in the channel the entity of the pressure drop will depend effectively on the geometry of the channel and its length. For this reason fluxes under the rib will be influenced themselves by the channel's dimension and shape. The serpentine design has elevated velocity along the edges of the flow field, particularly over the lands where the high pressure drop of the switchbacks forces the electrolyte to jump over the lands and through the electrode material to reach the outlet. This can be seen also in Figure 7 where the distribution of the reaction rate is concentrated in the zones mentioned. When the cell is operating in a lower state of charge, what happens is that some zones will be more influenced by mass transport problems as the concentration of the reactants might be an issue in the porous electrode, limiting the current generation process.

A graphical interpretation of under the rib fluxes is mentioned in Figure 11. The role of these fluxes is very important as they bring fresh electrolyte under a zone, the rib, where the potential is fixed. These two conditions push the reaction rate to higher values and convert the vanadium with higher volumetric rate. According to the researches, not much effort has been done to couple locally the performance of the cell and its fluid dynamic behaviour and no cases in the literature analyze such trends. For this reason Figures 10, 11 and 12 represent a tiny innovation to the approach of this problem regarding flow batteries. In Figures 12-14, reaction rate, state of charge and overpotential are shown on the left axis while on the right axis the scaled velocity is shown. The inlet is corresponding to *x/L* equal to zero and the outlet is one. From the beginning to the outlet of the cell state of charge decreases but in the zones where the velocity is higher also the state of charge increases.

The reaction rate is higher for the under the rib zones but the overpotential has a lower absolute value. What happens in this zone is that the absolute value of the volumetric rate 5.6 is pushed to higher values not by the overpotential but by the higher concentration of

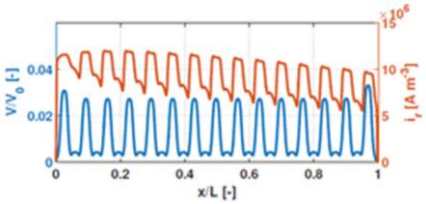

Figure 12. Reaction rate on the right axis, scaled velocity on the left axis

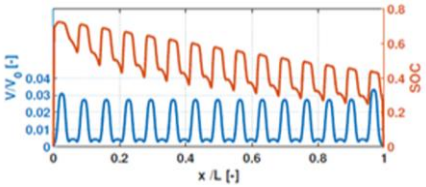

Figure 13. State of charge on the right axis, scaled velocity on the left axis

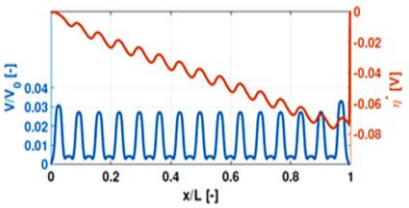

Figure 14. Overpotential on the right axis, scaled velocity on the left axis

reactants brought in this position by the under the rib flux from a fresh solution. The overpotential is a measure of the electrochemical loss in the battery from the inlet to the outlet and the absolute value of it decreases as, since the state of charge of the battery is decreasing, the losses to convert reactants increase.

To end this analysis a visualization of the under the rib fluxes is reported along with the values for the reaction rate. The distribution of the two quantities is important to locally characterize the mass transport phenomena and the electrochemical performance.

5. CONCLUSION

This work clarifies, according to the assumptions made, the phenomenon of the under the rib fluxes, visualizing this quantity inside the electrode domain. Not much effort has been done to relate locally the performance of the cell to the fluid dynamic condition whereas in this work this aspect is analyzed. In the serpentine channel, the pressure distribution inside the cell is heavily influenced by the geometry of the flow field and forces some fluid to pass under the rib in certain zones close to the switchbacks. The analysis of the under the rib fluxes pointed also out that locally the concentration of reactants is crucial for the capability of the system to operate with high current densities. The geometrical

characteristics of the domain have been investigated performing a sensitivity analysis with respect to the channel dimension pointing out that for a serpentine flow field the smaller the channel the higher the performance and the pressure drop for a given flow rate and state of charge. According to the experimental analysis present in the literature, a parallel flow field is presented as an example of a situation in which mass transport phenomena are l, imiting heavily the performance of the battery.

6. REFERENCES

1. Divya, K.C., Ostergaard, J., "Battery energy storage technology for power systems—an overview", ***Electric Power Systems Research***, Vol. 79, (2009), 511–520.
2. Dhassa, A. D., Natarajana, E., Lakshmi, P., "an investigation of temperature wffects on solar photovoltaic cells and modules", ***International Journal of Engineering***, Transaction C: Aspects Vol. 27, (2014), 1713-1722.
3. Alotto, P., Guarnieri, M., Moro, F., "Redox flow batteries for the storage of renewable energy: A review", ***Renewable & Sustainable Energy Reviews***, Vol. 29, (2014), 325–335.
4. Ponce de Leon, C., Frıas-Ferrer, A., Gonzalez-Garcıa, J., Szanto, D.A., Walsh, F.C., "Redox flow cells for energy conversion", ***Journal of Power Sources***, Vol. 160, (2006), 716–732.
5. Kear, G., Shah, A.A., Walsh, F.C., "Development of the all vanadium redox flow battery for energy storage: a review of technological, financial and policy aspects", ***International Journal of Energy Research***, Vol. 36, (2011), 1105-1120.
6. Skyllas-Kazacos, M., Chakrabarti, M.H., Hajimolana, S. A., Mjalli, F.S., Saleem, M., "Progress in Flow Battery Research and Development", ***Journal of The Electrochemical Society***, Vol. 158, (2011), 55-79.
7. Weber, A.Z., Mench, M.M., Meyers, J.P., Ross, P.N., Gostick, J.T., Liu, Q., "Redox flow batteries: A review", ***Journal of Applied Electrochemistry***, Vol. 41, (2011), 1137–1164.
8. Xu, Q., Zhao, T.S., Leung, P.K., "Numerical investigations of flow field designs for vanadium redox flow batteries", ***Applied Energy***, Vol. 105, (2013), 47–56.
9. Kim, D. K., Yoon, S. J., Lee, J., Kim, S., "Parametric study and flow rate optimization of all-vanadium redox flow batteries", ***Applied Energy***, Vol. 228, (2018), 891-901.
10. Yin, C., Gao, Y., Guo, S., Tang, H., "A coupled three dimensional model of vanadium redox flow battery for flow field designs", ***Energy***, Vol. 74, (2014), 886–895.
11. Xu, Q., Zhao, T.S., "Fundamental models for flow batteries", ***Progress in Energy and Combustion*** Science, Vol. 49, (2015), 40–58.
12. Shah, A.A., Watt-Smith, M.J., Walsh, F.C., "A dynamic performance model for redox-flow batteries involving soluble species", ***Electrochimica Acta***, Vol. 53, (2008), 8087–8100.
13. You, D., Zhang, H., Chen, J., "A simple model for the vanadium redox battery", ***Electrochimica Acta***, Vol. 54, (2009), 6827–6836.
14. Pugach, M., Kondratenko, M., Briola, S., Bischi, A., "Zero dimensional dynamic model of vanadium redox flow battery cell incorporating all modes of vanadium ions crossover", ***Applied Energy***, Vol. 226, (2018), 560-569.
15. López-Vizcaíno, R, Mena, E, Millán, M, Rodrigo, M, Lobato, J, "Performance of a vanadium redox flow battery for the storage of electricity produced in photovoltaic solar panels", ***Renewable Energy***, Vol. 114, (2017), 1123-1133.
16. Suresh, S., Ulaganathan, M., Venkatesan, N., Periasamy, P., Ragupathy, P., "High performance zinc-bromine redox flow batteries: Role of various carbon felts and cell configurations", ***Journal of Energy Storage***, Vol. 20, (2018), 134-139
17. Yan, Y., Skyllas-Kazacos, M., Bao, J, "Effects of battery design, environmental temperature and electrolyte flowrate on thermal behaviour of a vanadium redox flow battery in different applications", ***Journal of Energy Storage***, Vol. 11, (2017), 104-118.
18. Li, Y., Zhang, X., Bao, J., Skyllas-Kazacos, M., "Studies on optimal charging conditions for vanadium redox flow batteries", ***Journal of Energy Storage***, Vol. 11, (2017), 191-199.
19. Bhattacharjee, A, Saha, H, "Development of an efficient thermal management system for Vanadium Redox Flow Battery under different charge-discharge conditions", ***Applied Energy***, Vol. 230, (2018), 1182-1192
20. Nield, Donald A., and Adrian Bejan. Convection in porous media. Vol. 3. New York: springer, 2006.

A Numerical Simulation of Vanadium Redox Flow Batteries

P. Hasannasab, A. A. Ranjbar, M. Shakeri

Mechanical Engineering Department, Babol Noshirvani University of Technology, Babol, Iran

P A P E R I N F O

Paper history:
Received 30 November 2018
Received in revised form 29 December 2018
Accepted 03 Januray 2019

Keywords:
Flow Fields
Pressure Loss
All Vanadium Redox Flow Battery
Numerical Simulation

چکیده

تحقیقات اخیر برروی سیستمهای انرژی تجدید پذیر باعث گسترش نیاز به سیستمهای تولید انرژی پراکنده بمنظور تولید انرژی، تعادل و یا تقویت برق شبکه شده است. در میان سیستمهای الکتروشیمیایی ذخیره انرژی، باتری‌های جریانی وانادیومی قابل اتکاترین و پربازده‌ترین آنها با طول عمر بالا می‌باشد. البته با توجه به چگالی انرژی پایین و هزینه بالا فعلی، همچنان جای بهبود و گسترش روی این سیستم‌ها بسیار مطرح می‌باشد. در این مقاله یک میدان مارپیچ جریان بر اساس سیستم‌های شبیه سازی عددی برروی یک باتری جریانی ردوکس وانادیومی مورد بررسی قرار می‌گیرد. ارتقا روی مدل سه بعدی بخش کاتد در این باتری‌ها مطرح می‌گردد. نتایج بر نوع پخش واکنش، پتانسیل اضافی، سرعت و میزان شارژ باتری شامل یک سلول نشان داده شده است.

***doi**: 10.5829/ije.2019.32.01a.20*